Experimental Study of Current Filamentation Instability

B. Allen, V. Yakimenko, M. Babzien, M. Fedurin, K. Kusche, and P. Muggli

Phys. Rev. Lett. **109**, 185007 — Published 2 November 2012

DOI: 10.1103/PhysRevLett.109.185007

Experimental Study of Current Filamentation Instability

B. Allen[1*] and V. Yakimenko[2], M. Babzien[2], M. Fedurin[2], K. Kusche[2], P. Muggli[3,1]

[1] *University of Southern California, Los Angeles, CA 90089, USA*

[2] *Brookhaven National Laboratory, Upton, NY 11973, USA*

[3] *Max Planck Institute for Physics, Munich, Germany*

Abstract

Current filamentation instability is observed and studied in a laboratory environment with a $60MeV$ electron beam and a plasma capillary discharge. Multiple filaments are observed and imaged transversely at the plasma exit with optical transition radiation. By varying the plasma density the transition between single and multiple filaments is found to be $k_p\sigma_r \sim 2.2$. Scaling of the transverse filament size with the plasma skin depth is predicted in theory and observed over a range of plasma densities. Lowering the bunch charge, and thus bunch density, suppresses the instability.

* brianall@usc.edu

The interaction of particle beams with plasmas is a research topic relevant to many fields of physics, from the microscopic to the astrophysical world. In particular, relativistic particle beams propagating in plasmas are subject to the current filamentation instability (CFI) [1] that breaks up the beam into narrow and high current filaments and thereby generates or enhances magnetic fields. The interaction of the relativistic particles with these magnetic fields leads to the emission of synchrotron radiation and can also strongly modify the particle's trajectories and alter the transport of energy and momentum.

The Inertial Confinement Fusion - Fast Igniter concept (ICF) [2] relies on a beam of hot electrons created by the short, intense laser pulse at the critical density surface to propagate through the dense plasma and deposit its energy at the core of a partially compressed fuel pellet. These hot electrons ignite the fusion process with reduced compression requirements, compared to the original ICF concept. The electron beam generates a strong plasma return current and is subject to CFI [3]. The occurrence of CFI could modify and limit the energy deposition processes and prevent ignition.

In astrophysics, the phenomena responsible for the afterglow radiation following Gamma Ray Bursts (GRB's) are largely unknown. One proposed theory for the afterglow is the Fireball theory [4]. In this theory, matter consisting of electrons, positrons and ions is ejected from the supernova. Although potentially neutral, these flows of charged particles interact with the interstellar plasma medium and are subject to CFI. The instability leads to currents and magnetic fields generation as well as to the emission of radiation. It can also be the precursor to the generation of collisionless relativistic shocks.

In plasma wakefield accelerators CFI imposes a limit on the maximum plasma density and therefore on the maximum accelerating gradient that can be reached with a bunch focused to a given size. This is particularly important for the proton-driven PWFA experiments in the long bunch regime that are in preparation at CERN where the plasma density will be kept below $10^{15} cm^{-3}$ in order to avoid the development of CFI in the bunch focused to $200 \mu m$.

It is therefore both interesting and important to demonstrate in the laboratory that CFI can indeed occur with the predicted beam and plasma parameters.

The occurrence of CFI has been postulated in the context of laser-driven, plasma-based accelerators [5, 6]. However, these experiments did not study the basic features of the instability including the transition from single to multiple filaments and scaling of the filament's

size with plasma density nor have they shown transverse imaging of the filaments.

In this *Letter* we report for the first time the observation of multiple beam filaments resulting from CFI of a well controlled accelerator electron bunch propagating in plasmas at various densities. We show that as expected from an instability, the number and size of the filaments vary from event to event. However, we also show that, as expected from theory, multiple filaments are observed only when the transverse bunch radius (σ_r) is large when compared to the cold plasma collisionless skin depth (c/ω_{pe}): $\sigma_r/(c/\omega_{pe}) > 1$. The transition is observed at $\sigma_r/(c/\omega_{pe}) = 2.2$. We also show that, on average, the size of the filaments scales with c/ω_{pe}, and that at lower bunch densities, all else constant, CFI does not occur. It is important to note that the basic features of CFI are observed despite deviation from the ideal parameters studied in theory and simulations. These deviations include a finite size beam, finite beam emittance (temperature) and a Gaussian charge distribution. Particle in cell numerical simulations with beam and plasma parameters similar to those of the experiment confirm the observations reported here.

Current Filamentation Instability, CFI, is a basic charged particle beam-plasma instability that is purely transverse electromagnetic and has a purely imaginary frequency. It occurs due to non-uniformities in the beam current density and plasma return current density. These opposite currents enhance the beam magnetic field. The resulting $\vec{v} \times \vec{B}$ force, $\vec{v}$ - velocity of the beam or plasma particles and $\vec{B}$ - magnetic field, amplifies the currents' non-uniformities and drives the instability. As a result the bunch breaks up in the transverse plane into larger current density filaments with size and spacing on the order of the plasma skin depth, c/ω_{pe}, c - speed of light in vacuum, $\omega_{pe} = \sqrt{\frac{n_e e^2}{m_e \varepsilon_o}}$ - electron plasma frequency, n_e - plasma electron density, e, m_e - electron charge and mass and ε_o - permittivity of free space. When the filaments reach this typical size the instability saturates. At this point the filaments do not focus any more and the high space charge and larger emittance dominate and the filaments first defocus and then merge. For CFI to occur the beam particle's transverse temperature or the beam emittance must be low enough such that the effect of the plasma on the beam is not compensated by the emittance, an effect that has been observed in simulations [7].

For particle beams with finite transverse extent, the regime where CFI can occur is determined by two parameters, (1) the transverse bunch size relative to the plasma skin depth and (2) the Lorentz factor, γ_o, of the beam. For the case where the transverse beam

size is smaller than the plasma skin depth $\sigma_r < c/\omega_{pe}$, or $k_p\sigma_r < 1$, $k_p = \omega_{pe}/c$ - plasma wavenumber, the plasma return current flows outside the bunch, this is a regime particularly favorable for Plasma WakeField Accelerators (PWFA) [8, 9] and CFI does not occur. When the transverse bunch size is larger than the plasma skin depth, $k_p\sigma_r \gg 1$, the return current flows through the bunch, creating a situation where CFI can occur. In general, the beam is subject to instabilities with a wavenumber, $\vec{k}$, at an arbitrary angle with respect to the bunch propagation velocity, $\vec{v_b}$. Linear analysis [10] reveals that for low γ_o beams, the dominant instability is a two stream electrostatic instability with $\vec{k} \| \vec{v_b}$. For relativistic beams, $\gamma_o \gg 1$, CFI with $\vec{k} \perp \vec{v_b}$ is the dominate instability. Simulations reveal that for the finite transverse beam size case ([10] is for the case of an infinite transverse beam size) CFI dominates and the filament size and spacing are on the order of the plasma skin depth [11]. The growth rate, Γ, of the instability is [12]:

$$\Gamma = \beta_o \sqrt{\frac{\alpha}{\gamma_o}} \omega_{pe} = \beta_o \sqrt{\frac{n_b e^2}{\gamma_o m_e \varepsilon_o}} \tag{1}$$

$\beta_o = v_b/c$ - velocity ratio, $\alpha = n_b/n_e$ - density ratio and n_b - electron bunch density. Equation 1 shows that the CFI growth rate, in the infinite case, scales with the bunch density, $\propto \sqrt{n_b}$, and is independent of the plasma density, providing that $k_p\sigma_r \gg 1$.

The experiment was performed at Brookhaven National Laboratory's Accelerator Test Facility (ATF) with the linear accelerator that produces $\sim 60MeV$ ($\gamma_o \simeq 117$) root mean squared (RMS) electron bunches of length $\simeq 5ps$ and a charge of $Q \sim 1.0nC$. For these experiments the beam is focused near the plasma entrance to transverse sizes $\sigma_{0x,y}$ between 45 and $100\mu m$. The normalized beam emittance is $\epsilon_N \sim 4 - 8mm \cdot mrad$. The plasma is created with a hydrogen capillary discharge [13] of length $L_p = 2cm$ and diameter of $\sim 1mm$. The backing gas pressure is $110Torr$ and the applied voltage is $15kV$. Plasma densities of $10^{13} < n_e < 7 \times 10^{17} cm^{-3}$, corresponding to $6 < c/\omega_{pe} < 2,300\mu m$, are achievable. The plasma density at three positions along the capillary is derived from Stark broadening by measuring the linewidth of the Balmer H_α line [14] versus time. The three densities are within 10% of each other [15]. The plasma density, and hence the plasma skin depth, is selected by varying the delay between the plasma generation time and the electron bunch arrival time at the plasma/capillary entrance.

The experimental setup is shown in Figure 1. We use optical transition radiation (OTR) for the imaging of the bunch and filaments in the plane transverse to the beam propagation.

The electrons emit OTR when exiting a $100\mu m$ thick Si window [16] coated with a $\approx 200nm$ thick layer of Au. The window is placed directly at the capillary exit. It terminates the plasma and prevents propagation of the filaments in the downward plasma ramp that would exist otherwise. Simulations indicate that in the ramp the filaments would merge over a very short distance due to their small transverse size and larger emittance. The scattering angle of the 60MeV electrons in the $dx = 100\mu m$ thick Si window is $\theta \cong 6mrad$ and results in an increase in filament size on the order of $\Delta\sigma_{0x,y} = \theta dx \sim 0.6\mu m$. This size increase is small compared to the smallest filament sizes expected in the experiment, on the order of $c/\omega_{pe} \sim 6\mu m$ at the highest plasma density and is neglected in the analysis presented below. The OTR light is collected with a microscope objective and relayed out of the vacuum chamber onto an Electron Multiplying - Charged Coupled Device (EMCCD) camera. The measured optical resolution, USAF 1951 target, is $3.9\mu m$ RMS in the x and y directions, sufficient to measure the smallest expected filament size.

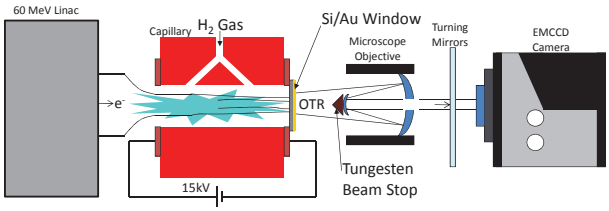

FIG. 1. Experimental setup: electron bunch from a $60MeV$ linac is focused to its waist at the entrance to the capillary. The plasma is generated by puffing H_2 gas at $110Torr$ into a $1mm$ diameter by $2cm$ long capillary with an applied voltage of $15kV$. OTR is generated from the bunch/filament electrons and the Au coating. The resulting light is collected and magnified by a microscope objective and relayed with turning mirrors out of the vacuum chamber to an EMCCD camera.

The characteristic expansion length of the electron beam from its waist is given by its beta function $\beta_{0x,y} = \gamma_0\sigma_{0x,y}^2/\epsilon_N > 3cm$ and $\beta_{0x,y} \gg L_p$. Thus, the size measurements at the plasma exit for events without plasma can be taken to be the same as at the capillary entrance and used as the input condition for events with plasma. The incoming bunch x and y profiles without plasma are essentially Gaussian and characterized by their RMS sizes σ_{0x} and σ_{0y}. Measurements show that in general the bunch transverse size $\sigma_{0x,y}$ does not vary by more than 10% RMS from event to event and over a typical measurement period.

Data collection includes alternately recording transverse images of the bunch at the plasma/capillary exit with (filamented beam) and without plasma (incoming beam). The relative charge of the electron bunch in the accelerator and the discharge current and plasma light time evolution are recorded for every event. The relative bunch charge is calibrated with a Faraday cup upstream of the capillary. Two types of plasma density scans were used for data acquisition. Continuous scans, to study the evolution of the instability as a function of $k_p\sigma_{0x,y}$, record one event at 55 different densities over the full plasma density range. Discrete scans, to study the scaling of the filament size with plasma skin depth and to capture the variations due to the instability nature of the interaction. Ten events were recorded at six different plasma densities with $9 < c/\omega_{pe} < 42\mu m$.

We define the occurrence of CFI to be when multiple filaments are observed with the plasma and when on average, the filament size scales with the plasma skin depth. As the plasma density is decreased such that $k_p\sigma_{0x,y} < 1$ we expect only single "filament" events. Note that reduction of the bunch transverse size at the plasma exit with $k_p\sigma_{0x,y} < 1$ can be interpreted as plasma focusing by the underdense plasma [17]. Further, we expect CFI not to occur when the bunch density is reduced while keeping $k_p\sigma_{0x,y}$ constant, as suggested by the CFI growth rate (Eq. 1). However, plasma focusing remains, simply with a different reduction in transverse size and does not scale directly with c/ω_{pe} but with the bunch charge.

One representative transverse bunch image without plasma and five images with plasma and exhibiting focusing or filamentation are shown in Figure 2. In practice we identify a filament as a high count feature in the images. For these events the electron bunch parameters are $\sigma_{0x} \sim 80\mu m$ and $\sigma_{0y} \sim 50\mu m$, charge $Q \sim 1.0nC$ and the plasma skin depth and values of $k_p\sigma_{0x}$ and $k_p\sigma_{0y}$ are $41.6\mu m$, ~ 1.9, ~ 1.2 for Fig. b, $15.4\mu m$, ~ 5.2, ~ 3.3 for Figs c and d and $12.3\mu m$, ~ 6.5, ~ 4.1 for Figs e and f, respectively. Figure 2 has b) 1, c) 5, d) 3, e) 3 and f) 4 filaments respectively. Note that in all cases, Figs 2 b) to f), the features identified as filaments have a higher peak count than the incoming bunch, Fig. 2 a), and therefore larger current densities. The total count is conserved for events with and without plasma to an average difference of 14%. These images illustrate the random character of the instability. The filaments size, position and number change with plasma density (see below). They also change from event to event, even with similar experimental conditions, a typical behavior for an instability-driven interaction.

Figure 3 shows again the instability nature of the bunch filamentation through the number

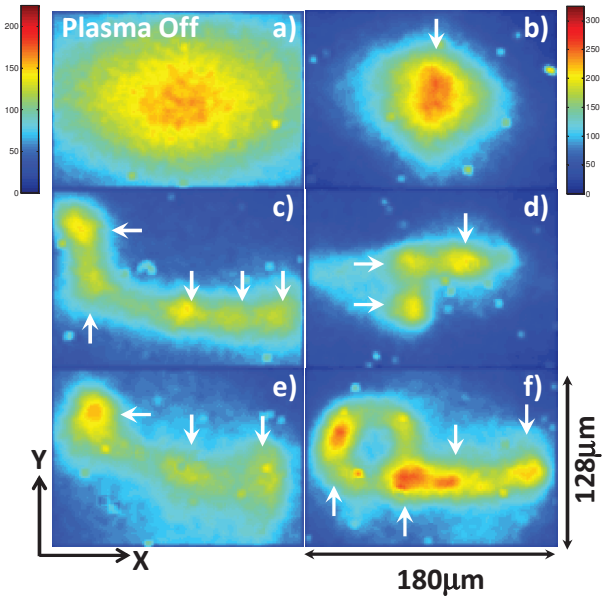

FIG. 2. OTR images of the bunch at the capillary exit with arrows indicating filaments. Bunch parameters are $\sigma_{0x} \sim 80\mu m$, $\sigma_{0y} \sim 50\mu m$ and charge $Q \simeq 1.0nC$. a) without plasma and b) $n_e = 1.6\text{x}10^{16} cm^{-3}$ $(c/\omega_{pe} = 41.6\mu m)$, c) and d) $n_e = 1.2\text{x}10^{17} cm^{-3}$ $(c/\omega_{pe} = 15.4\mu m)$ and e) and f) $n_e = 1.9\text{x}10^{17} cm^{-3}$ $(c/\omega_{pe} = 12.3\mu m)$. X-rays are seen in the images and are a few pixels in size. Color tables are the same for b) through f).

of filaments observed at various plasma densities, but displayed as a function of $k_p\sigma_{0y}$. To locate the transition from single filament events, expected for $k_p\sigma_{0y} < 1$, to multiple filament events, expected for $k_p\sigma_{0y} > 1$, from a large data set both the continuous and discreet scan data is used. Additionally, we recorded 120 events at $k_p\sigma_{0y} \sim 4.1$ that showed between one and four filaments. Therefore single points in Fig. 3 in general correspond to multiple events with the same number of filaments. There is a very clear transition between single and multiple filaments occurrences around $k_p\sigma_{0y} \sim 2.2$. Most noticeably there are no cases of multiple filaments for $k_p\sigma_{0y} < 2.2$. Some instances of single filaments are present for $k_p\sigma_{0y} > 2.2$, but the number of filaments can be as large as five. This variability is attributed to the sensitivity of the CFI to slight changes in plasma and bunch initial conditions. For $k_p\sigma_{0y} > 4.5$ only one or two filaments are observed, which could be due to the merging of filaments [7]. This merging is also seen in simulations even though Eq. 1 shows the growth rate is independent of plasma density.

The RMS transverse filament sizes is determined from x and y projections by selecting

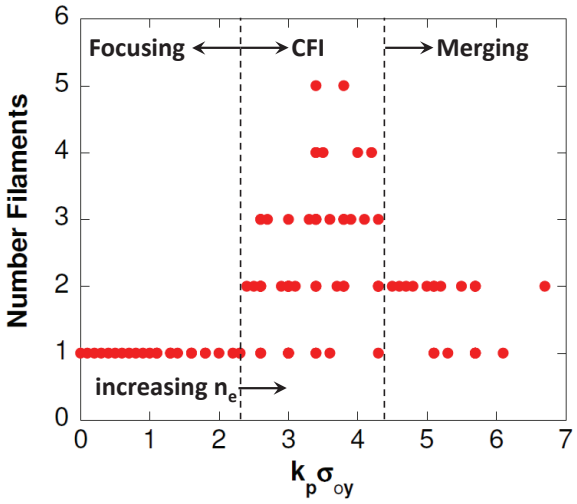

FIG. 3. Number of filaments observed in single events as a function of the CFI parameter $k_p\sigma_{0y}$. For this measurement the charge $Q \simeq 1.0nC$ and $\sigma_{0x} \sim 80\mu m$, $\sigma_{0y} \sim 50\mu m$. Similar events lead to only single filaments for $k_p\sigma_{0y} < 2.2$ and multiple (one to five) filaments for $k_p\sigma_{0y} > 2.2$. For $k_p\sigma_{0y} > 4.5$ only one and two filaments are seen and could be due to merging of filaments. In general single points represent multiple events at the same $k_p\sigma_{0y}$.

a small region around the features identified as filaments. On a scan to scan basis the number of available (symmetric profiles) x and y filament projections for multiple filament events depends on the location of the filaments, see Fig. 2. The data set used was selected based on the largest number of available x or y projections for multiple filament events. For example, in Fig. 4 there are 29 and 13 available x and y projections respectively and the x projections were used. Root mean squared filament sizes measured with the incoming bunch sizes $\sigma_{0x} = 81\mu m$ and $\sigma_{0y} = 53\mu m$ and charge $Q \simeq 1.0nC$, named high charge, are shown in Figure 4. For this scan, multiple filaments, one to five, were observed for $9 \leq c/\omega_{pe} \leq 20\mu m$ corresponding to $2.7 < k_p\sigma_{0y} < 5.8$ on Figure 3, that is over about one decade in plasma density. On average the filament size scales with the plasma skin depth for $12 \leq c/\omega_{pe} \leq 42\mu m$. For the skin depth $< 10\mu m$, the highest plasma density, the filaments size is larger than c/ω_{pe}, which could be due to merging of the filaments.

The growth rate of the instability scales as $\propto \sqrt{n_b} = [Q/(e(2\pi)^{3/2}\sigma_{0x}\sigma_{0y}\sigma_{0z})]^{1/2}$ (see Eq. 1) and reducing the bunch charge reduces the development of CFI. The high charge scan in Figure 4 was repeated with half the charge, $Q \sim 0.54nC$, and approximately the

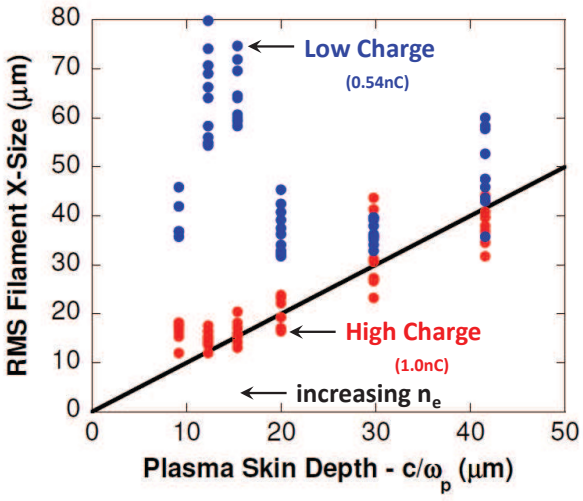

FIG. 4. Transverse filament size (RMS): red markers high charge scan - $Q \simeq 1.0nC$ and $\sigma_{0x} = 81\mu m$, $\sigma_{0y} = 53\mu m$. Blue markers low charge scan - $Q \simeq 0.54nC$ and $\sigma_{0x} \simeq 89\mu m$, $\sigma_{0y} \simeq 45\mu m$. Both scans consist of six different plasma densities with each ten events recorded. The solid line represents exact correlation between filament size and plasma skin depth.

same transverse bunch profile, $\sigma_{0x} \sim 89\mu m$ and $\sigma_{0y} \sim 45\mu m$ and is shown in Figure 4. Evaluation of the growth rate given in Eq. 1 with the high charge bunch indicates a growth of the CFI by 2.7 e-folding over the 2-cm long plasma and 2.1 e-folding for low charge bunch. This low charge scan generated only single filaments at all six plasma densities in contrast with the high charge scan where we observe one to five filaments for $c/\omega_{pe} \leq 20\mu m$. In addition, Fig. 4 shows that while the higher charge events follow the skin depth scaling (except at the highest plasma density as mentioned above) the low charge transverse sizes exhibit a completely different dependence on the skin depth. Data taken at even lower plasma densities, $100 < c/\omega_{pe} < 2,300\mu m$ (not shown here) for which $k_p\sigma_{0y} \ll 1$ shows that the dependencies of transverse bunch size on the plasma density are similar for the two charge cases with sizes consistently smaller in the higher charge case. Note that σ_{0y} varies by a larger amount at lower charge and explains the larger spread in filament size, 17% RMS compared to 10% RMS for high charge.

To summarize, we have presented experimental evidence of CFI in a laboratory setting with an electron beam and plasma capillary discharge under the parameters predicted in theory, $k_p\sigma_r \gg 1$ and a relativistic beam. The results are based upon transverse imaging of the filaments at the plasma exit with OTR. The transition from multiple to single filaments

was established, $k_p\sigma_r \sim 2.2$, by varying the plasma density through the CFI parameter $k_p\sigma_r$. We observed scaling of the filament size with the plasma skin depth over a range of plasma densities. Finally, we showed that by slowing the growth rate of CFI, by reducing the bunch density, CFI was not observed, either through multiple filaments or scaling with the plasma density.

We acknowledge useful discussions with T. Katsouleas. This work was supported by NSF grant 0903822 and DoE grant $DEFG03-92ER40745$. The contribution of the ATF technical staff to this work is greatly appreciated. Supporting numerical simulations were performed using the UCLA/IST consortium code QuickPIC on the USC/HPC cluster and NERSC computers.

---

[1] R. Lee and M. Lampe, Phys. Rev. Lett. 31, 23 (1973)

[2] M. Tabak et. al., Phys. Plasmas 1, (1994)

[3] Y. Sentoku et. al., Phys. Rev. Lett., 90, 15 (2003)

[4] G. Cavallo and M. J. Rees, Monthly Notices of the Royal Astronomical Society 183 (1978)

[5] M. Tatarakis et. al., Phys. Rev. Lett. 90, 17 (2003)

[6] C. M. Huntington et. al., Phys. Rev. Lett. 106, 10 (2011)

[7] J. J. Su et. al., IEEE Transactions on Plasma Science 15, 2 (1987)

[8] P. Chen et. al., Phys. Rev. Lett. 54, 693 (1985)

[9] I. Blumenfeld et. al., Nature 445, 7129 (2007)

[10] A. Bret, The Astrophysical Journal 699, 2 (2009)

[11] B. Allen et. al., AIP Conference Proceedings 1299, 1 (2010)

[12] A. Bret, M.-C. Firpo, and C. Deutsch, Phys. Rev. Lett. 94, 11 (2005)

[13] W. Kimura et. al., AIP Conference Proceedings 877, 2006

[14] J. Ashkenazy, R. Kipper, and M. Caner, Phys. Rev. A ,43 (1991)

[15] P. Muggli et al., AIP Conf. Proc. 1299 (2010)

[16] B. Allen et. al., PAC Conference Proceedings, 2011

[17] R. Keinigs and M. Jones, Phys. Fluids 30, (1987)